Molecular Pharmacology Fast Forward. Published on May 14, 2012 as DOI: 10.1124/mol.111.076752
This article has not been copyedited and formatted. The final version may differ from this version.

Telomere and Microtubule Targeting in Treatment-sensitive and Treatment-resistant Human Prostate Cancer Cells

Bin Zhang, Silke Suer, Ferenc Livak, Samusi Adediran, Arvind Vemula, Mohammad Afnan Khan, Yi Ning, and Arif Hussain

University of Maryland Greenebaum Cancer Center (B.Z., F.L., S.A., A.V., M.A.K, A.H.), University of Maryland School of Medicine, Baltimore, MD; Barbara Ann Karmanos Cancer Center (S.S.), Wayne State University School of Medicine, Detroit, MI; Department of Pathology (Y.N.), University of Maryland School of Medicine, Baltimore, MD; Baltimore Veterans Affairs Medical Center (A.H.), Baltimore, MD

Molecular Pharmacology Fast Forward. Published on May 14, 2012 as DOI: 10.1124/mol.111.076752
This article has not been copyedited and formatted. The final version may differ from this version.

Running Title: Telomere and Microtubule Targeting in Prostate Cancer

Corresponding Author: Arif Hussain,

22 S. Greene St

University of Maryland Greenebaum Cancer Center

Baltimore, MD 21201

Tel: 410-328-7225

Fax: 410-328-0805

Email: ahussain@som.umaryland.edu

Text pages: 41

Total Figures: 7

Tables: 2

References: 51

Abstract: 250

Introduction: 545

Discussion: 1357

ABBREVIATIONS: APL, acute promyelocytic leukemia; ATO, arsenic trioxide; BCRP, breast cancer resistance protein; CI, combination index; CRPC, castration resistant prostate cancer; CSC, cancer stem cells; DRI, drug reduction index; FISH, fluorescence in-situ hybridization; h-TERT, human telomere reverse transcriptase; PC, prostate cancer; Pgp, P-glycoprotein; RT-PCR, real time- polymerase chain reaction; SLC, stem-like cells; SP, side population; TRAP, telomeric repeat amplification protocol assay; TRF, telomere restriction fragment; VP, verapimil

Molecular Pharmacology Fast Forward. Published on May 14, 2012 as DOI: 10.1124/mol.111.076752
This article has not been copyedited and formatted. The final version may differ from this version.

ABSTRACT

Modulating telomere dynamics may be a useful strategy for targeting prostate cancer (PC) cells as they generally have short telomeres. As a plateau has been reached with taxane-based therapies in PC, this study was undertaken to evaluate the relative efficacy of targeting telomeres and microtubules in taxane-sensitive, taxane-resistant, androgen-sensitive and androgen-insensitive PC cells. Paclitaxel- and docetaxel-resistant DU145 cells were developed and their underlying adaptive responses evaluated. Telomere dynamics, and the effects of targeting telomeres with KML001 (sodium metaarsenite), an agent undergoing early clinical trials, were evaluated in parental and drug-resistant cells, including in combinations with paclitaxel and docetaxel. The studies were extended to androgen-sensitive LNCaP and androgen-insensitive LNCaP/C81 cells. Both P-glycoprotein (Pgp) and non-Pgp mechanisms of resistance were recruited within the same population of DU145 cells upon selection for drug resistance. *Wt* DU145 cells have a small side population (SP; 0.4-1.2%). The SP fraction increased with increasing drug resistance and correlated with enhanced Pgp but not Breast Cancer Resistance Protein (BCRP) expression. Telomere dynamics remained unchanged in taxane-resistant cells, which retained sensitivity to KML001. Further, KML001 targeted SP and non-SP fractions, inducing DNA damage signaling in both. KML001 induced telomere erosion and decreased telomerase gene expression, and was also highly synergistic with the taxanes in *wt* and drug-resistant DU145 cells. This synergism extended to androgen-sensitive and androgen-insensitive LNCaP cells under basal and androgen-deprived conditions. These studies demonstrate that KML001 with docetaxel or paclitaxel are highly synergistic drug combinations and should be explored further in the different disease states of PC.

Molecular Pharmacology Fast Forward. Published on May 14, 2012 as DOI: 10.1124/mol.111.076752
This article has not been copyedited and formatted. The final version may differ from this version.

Introduction

The microtubular network represents an important target for treating prostate cancer, particularly advanced castration resistant disease. Although the microtubule-targeting agent docetaxel has improved overall survival in men with metastatic prostate cancer, not all patients respond to it (Berthold et al., 2008; Petrylak et al., 2004; Tannock et al., 2004). Even for men who respond to docetaxel, the treatment is primarily palliative as most experience disease progression within a few months. To improve upon response rates and response duration, a number of agents have been evaluated in various combinations with docetaxel. However, to date, no docetaxel-based combination regimen has been shown to be superior to single agent docetaxel in castration resistant prostate cancer (CRPC) in phase III trials. Importantly, the overall landscape for patients with metastatic CRPC is beginning to gradually change with the recent approval of several therapies, including sipuleucel-T, cabazitaxel, abiraterone, and denosumab (de Bono et al., 2010; de Bono et al., 2011; Fizazi et al., 2011; Kantoff et al., 2010). Despite such progress, most men with metastatic prostate cancer are likely to eventually succumb to their disease.

With respect to taxanes, several mechanisms of inherent or acquired resistance have been implicated that likely contribute to their limited activity in prostate cancer (Greenberger and Sampath, 2006). Included among these resistance mechanisms are altered expressions of drug efflux pumps and/or qualitative changes in the microtubules themselves that potentially affect drug-target interactions.

Molecular Pharmacology Fast Forward. Published on May 14, 2012 as DOI: 10.1124/mol.111.076752
This article has not been copyedited and formatted. The final version may differ from this version.

We undertook the present study in an effort to better understand some of the adaptive responses of prostate cancer to the taxanes, and to identify new targets that could potentially be exploited for better therapeutic effect in both drug-sensitive and drug-resistant prostate cancer cells. Using DU145 cells as a model of androgen independent prostate cancer, a series of cell lines with varying levels of resistance to both paclitaxel and docetaxel were developed to study the adaptive responses to taxane selection. As telomere length maintenance is implicated in resistance to certain cytotoxic agents, we also investigated telomere dynamics in the above models (Burger and Harnden, 1998; Deschatrette et al., 2004; Ishibashi and Lippard, 1998; Mo et al., 2003; Multani et al., 1999; Smith et al., 2009). Since prostate cancer cells have short telomeres and hence may be particularly susceptible to telomere disrupting agents, we evaluated the role of targeting telomeres in both taxane-sensitive and taxane-resistant prostate cancer cells. These studies were extended to androgen-sensitive LNCaP and androgen-insensitive LNCaP/C81 cells.

In this report, we demonstrate that 1) considerable heterogeneity with respect to resistance mechanisms exists within the paclitaxel- and docetaxel-selected DU145 cell populations although they share a common phenotype of resistance to taxanes, 2) telomerase activity and telomere lengths are not significantly altered between drug-sensitive and drug-resistant DU145 cells, and they remain sensitive to a telomere targeting arsenical compound, KML001 ($NaAsO_2$, sodium metaarsenite), irrespective of the underlying resistance mechanisms, 3) KML001 can decrease telomerase gene expression and cause erosion of telomeres, and is synergistic with both paclitaxel and docetaxel in *wt* as well as highly taxane-resistant prostate cancer cells, and 4) this synergism extends to the androgen-sensitive LNCaP as well as the androgen-insensitive LNCaP/C81 cells under both basal and androgen-deprived conditions. These studies provide a

Molecular Pharmacology Fast Forward. Published on May 14, 2012 as DOI: 10.1124/mol.111.076752
This article has not been copyedited and formatted. The final version may differ from this version.

rationale for simultaneously targeting telomeres and microtubules in prostate cancer, including in treatment- naïve and treatment-resistant (chemotherapy- and castration-resistant) prostate cancer.

Molecular Pharmacology Fast Forward. Published on May 14, 2012 as DOI: 10.1124/mol.111.076752
This article has not been copyedited and formatted. The final version may differ from this version.

Materials and Methods

Cell Lines and Drugs. DU145 human prostate cancer cells were cultured in D-MEM/F12 medium (Invitrogen, Gaithersburg, MD) supplemented with 5% fetal bovine serum (FBS; Gemini, Calabasas, CA). LNCaP cells (passage number 30 or less) were cultured in RPMI-1640 medium supplemented with 10% FBS. LNCaP/C81 cells (designated C81) were provided by Dr. Anne Hamburger, University of Maryland Cancer Center; C81 are derived from LNCaP cells but have passage number >/= 81. The C81 cells were cultured in phenol red-free RPMI media supplemented with charcoal stripped serum (Gemini, Calabasas, CA). Paclitaxel-resistant DU145 cells were derived from parental DU145 cells by incremental exposure of the latter to increasing concentrations of drug. First, *wt* DU145 cells were exposed to 0.5 nM paclitaxel (IC50 dose). Surviving cells were then treated sequentially with increasing doses of paclitaxel over the course of several months to obtain DU145/Pac1, DU145/Pac10, and DU145/Pac200 cells whose final drug maintenance concentrations were 1, 10, and 200 nM paclitaxel, respectively. Docetaxel-resistant DU145 cells were obtained in a similar manner; these cells were designated DU145/Doc1, DU145/Doc10 and DU145/Doc60, and their final drug maintenance concentrations were 1, 10 and 60 nM docetaxel, respectively. The selected cells were cultured continuously in drug till the time of a particular experiment.

Paclitaxel (Bedford Laboratories, Bedford, OH) and docetaxel (Sanofi-Aventis Pharmaceuticals Products Inc., Bridgewater, NJ) stock solutions were obtained from University of Maryland Cancer Center Pharmacy. KML001 (sodium metaarsenite; Kominox) was provided by Komipharm International Co. Ltd. (Kyongki-Do, South Korea); 50 mM drug stocks were

prepared in PBS, and aliquots were stored at -20° C. The stock solutions were stable for more than one year. Working concentrations were freshly prepared.

Growth Inhibition Assays and Drug Combination Studies. The 3-[4,5-dimethylthiazol-2-yl]-2,5-diphenyltetrazolium bromide (MTT; Sigma-Aldrich Corp., St. Louis, MO) assay was used to assess the anti-proliferative effects of various drugs on our panel of cell lines per the method of Mosmann with minor modifications (Mosmann, 1983).

Drug combination studies were done according to the method of Chou and Talalay (Chou, 2008; Chou and Hayball, 1977; Chou and Talalay, 1984). Specifically, two-drug combinations were evaluated by the MTT assay over a range of concentrations by combining the drugs at their fixed IC_{50} ratios at each point tested. From these experiments, the combination index (CI) values at 50, 75 and 90% effective dose (ED50, ED75 and ED90, respectively), as well as drug reduction index (DRI) values, for each drug within the combination were determined using the CalcuSyn software program developed by Chou and Hayball (Chou and Hayball, 1977). According to this method, drugs are synergistic if the CI is < 1, additive if the CI is between 1 and 1.2, and antagonistic if the CI is above these values (Chou, 2008; Chou and Talalay, 1984).

Western Blot Analysis. Western blots were done as previously described using NuPAGE 4-12% Bis-Tris gels (Invitrogen, Gaithersburg, MD) to size fractionate cell lysates (Tang, 2006). Primary antibodies to the following proteins were used in the study: Pgp (MDR1) (Santa Cruz Biotechnology Inc., Santa Cruz, CA); BCRP, actin and β-tubulin (Sigma-Aldrich Corp., St. Louis, MO).

Molecular Pharmacology Fast Forward. Published on May 14, 2012 as DOI: 10.1124/mol.111.076752
This article has not been copyedited and formatted. The final version may differ from this version.

Side Population Assay, Cell Immunostaining and Cell Sorting. The side population (SP) assay was carried out according to the method of Goodell et al (Goodell et al., 1996). Cells were trypsinized and 0.5 x 10^6 cells resuspended in 1 ml medium containing Hoechst 33342 (5 µg/ml) alone, or Hoechst 33342 plus 50 µM verapamil (PgP inhibitor), or Hoechst 33342 plus 1 µM Ko143 (BCRP inhibitor, kindly provided by Dr. Nakanishi Takeo, University of Maryland Cancer Center). The cells were incubated at 37ºC for 90 minutes, spun down at 4 ºC for 5 minutes and then resuspended in cold Hanks' balanced salt solution **(**HBSS) (Invitrogen, Gaithersburg, MD) containing 2µg/ml propidium iodide (Invitrogen, Gaithersburg, MD). The samples were analyzed using a LSRI flow cytometer (BD Biosciences, San Jose, CA). Excitation of Hoechst dye with UV laser was at 350 nm and fluorescence was measured using a 450/20 BP filter (Hoechst blue) and a 675 EFLP optical filter (Hoechst red). Propidium iodide was excited with UV laser and fluorescence measured with 675 EFLP filter.

For immunostaining, trypsinized cells (0.5 x 10^6) were washed in HBSS with 2% fetal calf serum and 10mM HEPES buffer (HBSS+), and stained with APC mouse anti-human CD44 antibody (BD Pharmingen, San Diego, CA), phycoerythrin (PE)-conjugated Pgp antibody (Millipore, Temecula, CA), PE-conjugated mouse anti-human CD133 antibody (Miltenyi Biotec, Auburn, CA), FITC-conjugated CD49f antibody (Biolegend, San Diego, CA) and their respective controls. The cells were incubated in the dark on ice for 30 minutes, washed and then analyzed on a FACSCanto II (BD Bioscences, San Jose, CA) analytical flow cytometer. Data were analyzed using FlowJo software (TreeStar Inc., Ashland, OR).

Molecular Pharmacology Fast Forward. Published on May 14, 2012 as DOI: 10.1124/mol.111.076752
This article has not been copyedited and formatted. The final version may differ from this version.

Drug-resistant prostate cancer cells (20×10^6) were sorted two ways using a digital upgrade FACSVantage Diva cell sorter (BD Biosciences, San Jose, CA) according to whether or not they extruded the Hoechst 33342 dye (SP+ and SP- fractions), or using a FACSAria I cell sorter (BD Biosciences, San Jose, CA) based on whether or not they expressed Pgp on the cell surface (Pgp+ or Pgp- fractions). The gate for SP+ cells was set based on verapamil inhibition of Hoechst uptake by the treated cells. For sorting by Pgp status, cells were stained in HBSS+ containing either PE-conjugated Pgp antibody (1:50 dilution) or PE-conjugated isotype antibody (1:50 dilution) and incubated in the dark on ice for 30 min. After washing once in HBSS, Pgp expression was detected with a 488 nm laser and 576/26 BP filter; sorting gates were set with respect to isotype control staining which served as a negative base line.

Telomeric Repeat Amplification Protocol Assay. Telomerase enzyme activity was measured in cell extracts by the telomeric repeat amplification protocol (TRAP) assay using the TeloTAGGG-Telomerase PCR ELISA kit (Roche Diagnostics, Penzberg, Germany) according to the manufacturer's instructions and as we have reported previously (Burger, 2002). After adding stop solution, mean absorbance of the samples at 450 nm was determined using a microtiter plate reader (Synergy 2, Biotek, Winooski, VT).

Mean Telomeric Restriction Fragment Length (TRF) Analysis. Mean TRF lengths were determined using the TeloTAGGG-Telomere length kit as per the manufacturer's instructions. Genomic DNA was isolated using a DNA extraction kit (Qiagen, Hilden, Germany). 2 μg of DNA was digested with Hinf1 and Rsa1 for 2 hours at 37°C and loaded onto 0.8% agarose gels. The DNA was transferred to nylon membranes, hybridized to a digoxigenin-labeled telomere

Molecular Pharmacology Fast Forward. Published on May 14, 2012 as DOI: 10.1124/mol.111.076752
This article has not been copyedited and formatted. The final version may differ from this version.

probe, and the telomere related signals detected by chemiluminescence as described previously (Burger et al., 2005).

Real Time Polymerase Chain Reaction (RT-PCR). Total RNA was extracted from cells using QIAGEN RNeasy Mini Kit (QIAGEN, Valencia, CA) and purified by DNase digestion followed by elution in RNase free water. First strand cDNA was synthesized using iScript Select cDNA Synthesis Kit (Bio-Rad Laboratories Inc, Hercules, CA). Real time PCR was performed using 7900HT Fast Real-Time PCR System with Fast SYBR Green Master Mix (Applied Biosystems, Foster City, CA). Human telomerase reverse transcriptase (hTERT) primers (TIB Molbiol LLC, Adelphia, NJ) were 5'-ATGTCACGGAGACCACGTTT -3' (sense) and 5'-GGATGAAGCGGAGTCTGGAC - 3' (antisense). Human GAPDH primers were 5'-GGTGGTCTCCTCT GACTTCAACA-3′ (sense) and 5′-GTTGCTGTAGCCAAATTCGTTGT-3′ (antisense). The PCR reactions were done in triplicates. The PCR conditions included enzyme activation at 95ºC for 20 sec followed by 40 cycles of denaturing at 95ºC for 1 sec each and annealing/extension at 60ºC for 20 sec each. The specificity of the PCR reactions was verified by melting curve analysis. In the control samples no cDNA was added in the PCR reactions. hTERT gene expression was normalized with respect to GAPDH gene expression and analyzed by using the ΔΔCt method (Livak and Schmittgen, 2001).

Flourescence In-situ Hybridization (FISH). DU145 cells were cultured to 70% confluency and metaphase cells prepared by treating them with colcemid followed by hypotonic treatment and fixation. FISH was performed using a peptide nucleic acid (PNA) oligomer probe targeting the telomere repetitive sequence (PNA TelC-FAM probe; PNAbio Inc, Thousand Oaks, CA) as per

Molecular Pharmacology Fast Forward. Published on May 14, 2012 as DOI: 10.1124/mol.111.076752
This article has not been copyedited and formatted. The final version may differ from this version.

the manufacturer's instructions. Representative metaphase images were acquired using an Olympus Provis fluorescence microscope and an Applied Imaging system.

FISH using flow cytometry was performed per an established protocol (Baerlocher et al., 2006) with minor modifications. Briefly, trypsinized cells were split into four tubes ($2x10^5$ cells per tube), washed in hybridization buffer, and then resuspended in hybridization mixture (77 mM HEPES, 77 mM NaCl, 3.9% BSA, 29% deionized formamide) with 500 nM PNA TelC-FAM probe added to three of the four tubes. The tubes were incubated for 10 min at room temperature, then for 15 min at 87°C, followed by hybridization for 90 min at room temperature in the dark. The cells were washed four times and then resuspended in HBSS+. Flow cytometry was performed on a FACSCanto II cytometer, and the data were analyzed using the FlowJo software package. The mean fluorescence intensity (MFI) for each hybridized sample was calculated after subtracting background MFI (sample without probe). The resulting telomere fluorescence (the horizontal bars in histogram plots) was used to calculate the telomere lengths in the cells with respect to the known value of the untreated control.

Immunofluorescence. Approximately 1.5×10^4 to 2.0×10^4 cells were seeded into 8-well chamber slides over night. The cells were fixed and permeabilized by immersion three times for 1 minute each into ice-cold methanol/acetone (1:1) and dried for 15 minutes. The slides were blocked for 2 hours at RT with 5% BSA in PBS, incubated with Pgp mouse antibody or BCRP rabbit antibody or phospho-γ-H2AX mouse antibody (Millipore) at 1:200 dilution over night at 4°C, washed with PBS and further incubated for 2 hours with rabbit anti-mouse or goat anti-rabbit FITC (Sigma-Aldrich Corp., St. Louis, MO) at 1:200 dilution and then for 5 minutes with

Molecular Pharmacology Fast Forward. Published on May 14, 2012 as DOI: 10.1124/mol.111.076752
This article has not been copyedited and formatted. The final version may differ from this version.

DAPI (4,6-diamidino-2-phenylindole, 2 mg/ml; Sigma-Aldrich Corp., St. Louis, MO) at 1:5,000 dilution. After washing in PBS, the slides were mounted using Vectashield mounting media (Vector Laboratories, Burlingame, CA) and analyzed at 40x magnification with a Leica DM4000 microscope (Leica, Wetzlar, Germany) and 5.0 Openlab software (Perkin Elmer, Waltham, MA). Quantification of γ-H2AX foci induction was determined by measuring mean fluorescence intensity of at least 100 nuclei in each chamber.

Molecular Pharmacology Fast Forward. Published on May 14, 2012 as DOI: 10.1124/mol.111.076752
This article has not been copyedited and formatted. The final version may differ from this version.

Results

Paclitaxel- and Docetaxel-Resistant DU145 Prostate Cancer Cells. The IC_{50} values of paclitaxel and docetaxel for DU145 cells and the drug-resistant sublines are shown in Table 1. Exposure to increasing concentrations of a particular taxane (paclitaxel or docetaxel) results in increasing resistance not only to the selecting drug but also cross-resistance to the other taxane not used for the original selection (Table 1). Interestingly, it appears that the DU145 cells are prone to developing higher levels of resistance to docetaxel than to paclitaxel irrespective of the original taxane used for selection. For instance, DU145/Pac10 and DU145/Pac200 cells are 24- and 140-fold resistant, respectively, to paclitaxel (which was used to select them), but are 100- and 400-fold cross-resistant to docetaxel (Table 1). DU145/Doc10 and DU145/Doc60 cells are 100- and 500-fold resistant, respectively, to their selecting drug, i.e. docetaxel, but are only 24- and 100-fold cross-resistant to paclitaxel.

Both paclitaxel and docetaxel are known substrates of Pgp. This transporter is minimally expressed in *wt* DU145 cells but it becomes significantly over expressed in the taxane-resistant cells, particularly at the higher levels of drug selection (Fig 1a). The other ABC transporter, BCRP, is expressed in both *wt* and resistant cells, but its levels are not modulated with selection for resistance to the taxanes (Fig 1a). Flow cytometry reveals that Pgp is expressed on the cell surface of a significant fraction of the DU145/Pac200 (79% ± 6.5) and DU145/Doc60 (47 % ± 4.9) cell populations (Fig 1b). BCRP, on the other hand, is essentially undetectable on the surface of these cells (Fig 1b). This is further confirmed by immunohistochemistry, which

demonstrates cell surface localization of Pgp in DU145/Pac200 and DU145/Doc60 cells, but cytoplasmic localization of BCRP in both wt and taxane-resistant cells (data not shown).

'Side Population' and the Role of Pgp and BCRP in Taxane-Resistant Cells. The localization of Pgp to the surface of the DU145-derived cells suggests that the transporter is likely to be functional in them and hence contributes to their drug-resistant phenotype. By contrast, the cytoplasmic localization of BCRP suggests that it is not active in these cells, at least with respect to drug transport function. This is confirmed by flow cytometry using the 'side population' (SP) assay developed by Goodell et al (Goodell et al., 1996). The SP fraction is functionally defined by the extrusion of vital dyes such as Hoechst 33342 due to enhanced expression of ABC transporters (Goodell et al., 1996). The SP fraction can be enriched in stem/progenitor cells, and generally represents a very small portion of the total population; for instance it comprises approximately 0.1% of all nucleated cells in the bone marrow of mice, where it corresponds largely to hematopoietic stem cells.

Parental DU145 cells have a small SP fraction (0.4-1.2 %) (Fig 2a). This fraction increases in the cell lines selected for increasing resistance to docetaxel; it is approximately 20% in DU145/Doc10 and 60% in DU145/Doc60 cell populations, respectively (Fig 2a). Pgp-dependent exclusion of the dye was confirmed by treating these cells with verapamil (VP). Although VP is a potent inhibitor of L-type calcium channels, it also inhibits Pgp but not BCRP function. It has been used by investigators to assess Pgp-dependent transport (Tsuruo et al., 1981; Grossi and Biscardi, 2004). As seen in Fig 2b, VP inhibits extrusion of Hoechst 33342 from DU145/Doc10 and DU145/Doc60 cells, resulting in much higher uptake of the dye by them

Molecular Pharmacology Fast Forward. Published on May 14, 2012 as DOI: 10.1124/mol.111.076752
This article has not been copyedited and formatted. The final version may differ from this version.

(Fig 2b). The BCRP-specific inhibitor Ko143, on the other hand, has no effect on Hoechst 33342 uptake (Fig 2c). Taken together, these data demonstrate that it is primarily Pgp and not BCRP that is functional in the docetaxel selected DU145 cells, consistent with their respective plasma membrane and cytoplasmic localizations in these cells. Similar results are observed with the DU145/Pac series (not shown).

Since the SP fraction can contain stem-like cells, we also evaluated both the *wt* and paclitaxel- and docetaxel-resistant cells for the expression of several stem cell markers via FACS, including CD44, CD49f, and CD133. Anywhere from 28-66% of DU145 cells have been reported to be CD44+ by different investigators (Patrawala et al., 2006; Stuelten et al., 2010). In our hand, between78-88% of *wt* and taxane-resistant cells are CD44+ (Fig 3), while almost all of them appear to express CD49f on their cell surface (data not shown). Given the rarity of stem cells, only a small fraction of the above are likely to be 'stem-like' in our panel of cell lines, if they exist at all. Collins et al used another marker, CD133, to identify cancer stem cells in human prostate tumors; 0.1% of the prostate cells were found to be CD44+CD133+ and harbored a subpopulation with self-renewal properties (Collins et al., 2005). Among the DU145 cells, only a small fraction (0.87%) has been reported to be CD133+, which would be more consistent with the distribution pattern of a stem-like subpopulation (Stuelten et al., 2010). We were not able to identify a CD133+ subpopulation among either the *wt* or the taxane-resistant DU145 cells (Fig 3). Although we may be able to eventually detect some CD133+ cells with further optimization of our methods, importantly, our data suggest that taxane selection expands the SP population without significantly affecting the distribution pattern of any stem-like cells that might exist among the SP cells.

Molecular Pharmacology Fast Forward. Published on May 14, 2012 as DOI: 10.1124/mol.111.076752
This article has not been copyedited and formatted. The final version may differ from this version.

Analysis of Taxane-Resistant Cells Sorted by Flow Cytometry. It is apparent that in the total DU145/Doc10 and DU145/Doc60 cell populations (as well as among DU145/Pac10 and DU145/Pac200 cells) at least two subpopulations exist, one that is significantly modulated by VP in terms of Hoechst transport (SP subpopulation), and one that is minimally affected by VP (non-SP subpopulation). To further characterize these subpopulations, DU145/Pac200 cells were sorted into SP and non-SP fractions by flow cytometry to enrich for these fractions respectively. After cell sorting, 91% of total (or 98% of viable) cells in the SP fraction extruded Hoechst (Fig 4a, lower panel) compared to 65% of cells in the non-sorted parental DU145/Pac200 population (Fig 4a, upper panel). Similarly, the sorted non-SP fraction is enriched primarily for cells that do not extrude Hoechst (however, approximately 15% of the cells in the non-SP fraction can still extrude Hoechst, reflecting the limitations of cell sorting by such functional parameters). Fig 4b shows that Pgp expression in the non-SP fraction is significantly reduced compared to total and SP fractions of DU145/Pac200 cells. Thus, the non-SP and SP fractions are enriched for non-Pgp- and Pgp-expressing cells, respectively. Although the non-SP fraction has significantly reduced expression of Pgp, the IC_{50} values of the non-SP and SP fractions for paclitaxel are identical, demonstrating that both fractions are equally resistant to paclitaxel (Fig 4c).

We also sorted the parental DU145/Pac200 cells by cell surface expression of Pgp into Pgp+ and Pgp- fractions (Fig 4d, lower panel). Again, the IC_{50} values of the Pgp+ and Pgp- fractions for paclitaxel are identical (Fig 4e). Taken together, these data demonstrate that although all DU145/Pac200 cells have the same phenotype of resistance to paclitaxel, they can be associated with different mechanisms of resistance (i.e. Pgp and non-Pgp) within the same cell population

Molecular Pharmacology Fast Forward. Published on May 14, 2012 as DOI: 10.1124/mol.111.076752
This article has not been copyedited and formatted. The final version may differ from this version.

that is selected for drug resistance. Further, these Pgp- and non-Pgp-dependent pathways make the cells equally resistant to the selecting drug.

Telomeres, Telomerase Activity and Telomere Targeting in DU145-Derived Cells. Since telomere length maintenance is critical for chromosomal integrity, including in cancer cells, telomeres and telomerases are emerging as potentially important therapeutic targets (Olaussen et al., 2006). In addition to the well-defined property of targeting microtubules, paclitaxel has also been shown to cause erosion of telomeres in tumor cell lines (Mo et al., 2003; Multani et al., 1999). Therefore, we wanted to investigate the effects of targeting microtubules and telomeres in the DU145-derived cells. We have previously shown that KML001 is a telomere targeting agent, and its cytotoxic effects are telomere length dependent; cell lines with short telomeres (such as prostate cancer cells) are more sensitive to KML001 than those with longer telomeres (Phatak et al., 2008). The effects of paclitaxel and KML001 on parental DU145 cells were assessed by the SP assay (Fig 5a). In these experiments, approximately 1% of the DU145 cells are within the SP fraction. Paclitaxel at the IC_{50} and IC_{100} concentrations does not decrease the SP fraction of DU145 cells, although the total number of DU145 cells (primarily in the non-SP fraction) are reduced upon treating them with paclitaxel; this relative resistance of the SP subpopulation to paclitaxel is likely mediated by an ABC transporter present in SP cells (Fig 5a). By contrast, KML001 at IC_{100} can significantly reduce the SP fraction of DU145 cells (Fig 5a).

The IC_{50} values of KML001 for paclitaxel- and docetaxel-resistant DU145 cells are similar, or at most 2- to 3-fold higher, than for the drug-sensitive *wt* DU145 cells (Table 1). Since DU145/Pac200 cells have a large SP fraction that can be readily sorted by FACS, we also

Molecular Pharmacology Fast Forward. Published on May 14, 2012 as DOI: 10.1124/mol.111.076752
This article has not been copyedited and formatted. The final version may differ from this version.

evaluated the effects of KML001 on the sorted SP and non-SP fractions of DU145/Pac200 cells (Fig 5b-d). Fig 5b demonstrates that the SP (primarily Pgp-expressing) and non-SP (primarily non-Pgp-expressing) cells have similar IC_{50} values for KML001. Uncapping of telomeres can induce DNA damage signaling and response, including phosphorylation of γ-H2AX at Ser139, which represents an early event of DNA damage signaling (Phatak et al., 2008; d'Adda di Fagagna et al., 2003). KML001 induces phosphorylation of γ-H2AX in *wt* DU145 as well as DU145/Pac200 cells, including the SP and non-SP fractions, and if anything, more γ-H2AX phosphorylation occurs in the SP than the non-SP fractions (Fig 5c, d). Taken together, the above data demonstrate that, unlike paclitaxel, KML001 is a poor Pgp substrate, and can target both SP and non-SP cells.

Although modulating telomere dynamics represents a potentially attractive therapeutic strategy, alterations in telomerase activity and telomere lengths have also been implicated in resistance to certain cytotoxic agents (Burger and Harnden, 1998; Deschatrette et al., 2004; Ishibashi and Lippard, 1998; Smith et al., 2009). Therefore, we investigated whether any changes in telomerase activity and/or telomere lengths occurred in our panel of taxane-resistant prostate cancer cells. Telomere restriction fragment (TRF) length analysis showed that in the prostate cancer cells examined, including paclitaxel- and docetaxel-resistant lines, telomeres are short (2 to 3 kb) and essentially do not change as a consequence of drug selection (Table 1). Telomerase activity also does not change with selection for resistance to either paclitaxel or docetaxel (Table 1). Thus, although DU145 cells can be selected for high levels of resistance to the taxanes, their telomere dynamics are minimally affected, and they remain amenable to telomere targeting.

Molecular Pharmacology Fast Forward. Published on May 14, 2012 as DOI: 10.1124/mol.111.076752
This article has not been copyedited and formatted. The final version may differ from this version.

Importantly, when *wt* or DU145/Pac200 cells are treated with KML001, or paclitaxel, or a combination of the two at their respective IC50 values for 3 to 5 days, KML001 or the combination, but not paclitaxel alone, significantly reduces hTERT gene expression (approximately 5-fold; Fig 6a and data not shown). We also evaluated the relative integrity of telomeres in response to various treatments via FACS-coupled FISH. The ability of the FAM-labeled telomere-specific probe to detect telomeres in metaphase spreads of DU145 cells is shown in Fig 6b. It is apparent that a 72 hour incubation with KML001 or KML001 plus paclitaxel at IC50 concentrations leads to further telomere shortening, whereas paclitaxel alone has minimal effects (Fig 6c, d).

Combining KML001 with paclitaxel or docetaxel at their fixed IC_{50} ratios as per the method of Chou and Talalay to evaluate the dose-effect relationship of the drug combinations demonstrates that the highly resistant DU145/Pac200 cells become less resistant to either taxane in the presence of KML001. In fact, as shown in Fig 7, the combination index (CI) at the 50, 75 and 90% effective doses for KML001 plus paclitaxel or KML001 plus docetaxel in DU145/Pac200 cells is below 1, demonstrating synergism between KML001 and the taxanes. Overall, the CI values are also less than 1 in the *wt* DU145 cells and the resistant DU145/Doc60 cells, indicating synergism in these cell lines as well (Table 2). Also shown in Table 2 are the calculated dose-reduction index (DRI) values, which are a measure of the -fold reduction in dose of each drug in a combination to obtain the same therapeutic effect as with the individual drugs alone (Chou, 2008). Thus, for both *wt* and drug resistant DU145 cells a several fold reduction in paclitaxel or docetaxel dose is predicted when either is combined with KML001.

Molecular Pharmacology Fast Forward. Published on May 14, 2012 as DOI: 10.1124/mol.111.076752
This article has not been copyedited and formatted. The final version may differ from this version.

Studies in Androgen-Sensitive and –Resistant LNCaP Cells. LNCaP cells have been extensively studied as a cell culture model of androgen-sensitive prostate cancer. It is important to note that although androgen withdrawal inhibits their proliferation, such response of LNCaP cells to androgen deprivation is cell passage number dependent; LNCaP cells less than passage number 30 are androgen sensitive, whereas those greater than passage 81 (designated C81) maintain cell proliferation despite androgen withdrawal (Lin et al., 1998). Both LNCaP and C81 cells have a small SP fraction (approximately 0.6 and 0.2%, respectively), and do not appear to express Pgp or BCRP to any significant extent (Fig 1c). The IC_{50} values of paclitaxel, docetaxel and KML001 for LNCaP and C81 cells are listed in Table 1. Consistent with prior observations that androgen resistance can lead to relative chemoresistance, the C81 cells are 2- and 4-fold more resistant to docetaxel and paclitaxel, respectively, compared to LNCaP cells, but are equally sensitive to KML001 (Table 1). Both cell lines also have short telomeres and essentially identical telomerase activities (Table 1). For both LNCaP and C81 cells, the CI values for the KML001/paclitaxel or KML001/docetaxel combinations are less than 1 (Table 2). This demonstrates that KML001 is synergistic with either taxane in *both* LNCaP and C81 cells. However, the calculated DRI values suggest that LNCaP cells are more sensitive to the taxanes when they are combined with KML001 than C81 cells (Table 2).

Although at present we do not know the specific molecular pathway(s) contributing to the relatively lower DRI values for taxanes in C81 cells, recent studies regarding the mechanisms of arsenical and taxane action provide important insights that may account for some of the differences in sensitivities of the LNCaP and C81 cells to the KML001/taxane combinations. Two recent studies have identified additional effects of taxanes specifically in prostate cancer

Molecular Pharmacology Fast Forward. Published on May 14, 2012 as DOI: 10.1124/mol.111.076752
This article has not been copyedited and formatted. The final version may differ from this version.

(Zhu et al., 2010; Darshan et al., 2011). In particular, these studies have shown that microtubules play an integral role in the translocation of the androgen receptor (AR) from the cytoplasm to the nucleus (where it is active), and that disruption of microtubules by taxanes can impair AR activity in prostate cancer. Since LNCaP cells are more responsive/sensitive to the androgen-AR axis than C81 cells (Lin et al., 1998), this effect of taxanes on AR activity is likely to have a greater impact on LNCaP cells. Further, as arsenicals can also disrupt microtubule dynamics (Li and Broome, 1999; Ling et al., 2002; Cai et al., 2003), KML001 in combination with a taxane is likely to have a greater inhibitory effect in androgen-sensitive prostate cancer cells. Another recent intriguing action attributed to paclitaxel in prostate cancer cells is that it can enhance the interaction between AR and FOXO1, which inhibits AR function (Gan et al., 2009). Taken together, these mechanisms of taxane action are consistent with our observation regarding the prominent synergy between KML001 and taxanes in LNCaP cells, although this combination is also active in C81 cells but to a lesser extent (Table 2).

Molecular Pharmacology Fast Forward. Published on May 14, 2012 as DOI: 10.1124/mol.111.076752
This article has not been copyedited and formatted. The final version may differ from this version.

Discussion

One of the salient features of many cancers, particularly 'solid tumors', is their significant heterogeneity at the genetic and/or phenotypic levels, which likely contributes to the variable clinical course and outcomes to treatment among patients with seemingly similar tumor types. Further, it is becoming apparent that a small population of cells with stem-cell like properties, the so called cancer stem cells (CSC), exist within many tumors which can give rise to all the cells in the original tumor (Reya et al., 2001; Visvader and Lindeman, 2008). Conceivably, such CSC could potentially contribute to some of the tumor heterogeneity observed clinically.

The observed heterogeneity of clinical tumors is less apparent in established long term cancer cell lines, although cancer cells in culture can also demonstrate pleiotropic responses to selective pressure. With respect to taxanes, over expression of drug efflux pumps and/or mutations in beta-tubulin have been implicated as mechanisms that enable cancer cells to adapt to and survive taxane inhibition (Greenberger and Sampath, 2006). Our panel of DU145 cells up regulate Pgp in response to selection with both paclitaxel and docetaxel. Fig 1b reveals that the expression of Pgp at the cell surface varies among the different resistant cells that make up a particular paclitaxel- or docetaxel-selected population. Fig 1b further suggests that between 20 to 50% of the cells that make up the DU145/Pac200 or DU145/Doc60 populations, respectively, have minimal cell surface expression of Pgp. Studies evaluating Pgp transport function in the resistant cells show that only a fraction of DU145/Doc10 or DU145/Doc60 cells actually transport Hoechst 33342 (Fig 2), which is consistent with the proportion of Pgp-expressing taxane-resistant cells present in these populations.

Importantly, when the paclitaxel-resistant cells are sorted into SP (positive Hoechst 33342 transport) and non-SP (minimal/absent Hoechst 33342 transport) fractions, or into cell surface Pgp-positive or cell surface Pgp-negative fractions, the sorted fractions are equally resistant to paclitaxel (Fig 4). Thus, both Pgp and non-Pgp mechanisms of resistance may be associated with DU145 cells exposed to taxanes. Conceivably, an individual cell may employ one or more than one such mechanism of resistance. Such plasticity in response to taxane selection within the same DU145 cell population would not be apparent had only total cell lysates been analyzed by Western blots (e.g., Fig 1a). Stem-like cells (SLC) have also been identified in long term cancer cell line cultures, including in DU145 cells which have a small SP fraction (Figs 2a, 4a) (Stuelten et al., 2010). Whether these SLC contribute to the pleiotropic response to taxane-selection in DU145 cells, however, is presently not clear. Nevertheless, it is apparent from these studies that to improve upon the current taxane-based treatments in prostate cancer, strategies that address only Pgp-based resistance are unlikely to be successful. Rather, approaches that enhance the effects of taxanes, and also potentially address Pgp and non-Pgp resistance, and possibly SLC subpopulations, need to be developed.

We have previously shown that the telomere targeting agent KML001 is particularly active in cancer cell lines that have short telomeres, and is less so in those with longer telomeres (Phatak et al., 2008). Prostate cancer cell lines in general have relatively short telomeres and maintain endogenous telomerase activity, and thus are potential targets for telomere targeting agents (Phatak et al., 2008). It is important to note, however, that development of drug resistance can result in changes in telomere dynamics, including lengthening or shortening of telomeres and/or

changes in telomerase activity; such alterations appear to be dependent on cell type and the specific agents to which cells develop acquired resistance (Burger AM and Harnden, 1998; Deschatrette et al., 2004; Ishibashi and Lippard, 1998; Smith et al., 2009). Our panel of drug-resistant DU145 cells continue to maintain short telomeres irrespective of the taxane (paclitaxel or docetaxel) used for selection, or the levels of resistance acquired by the drug-selected cells (Table 1). Moreover, total telomerase activity does not appear to be altered between *wt* and taxane-resistant cells (Table 1), although it is up to 2-fold higher in the SP compared to the non-SP fractions of the highly resistant DU145/Pac200 cells (data not shown). Taken together, these data suggest that targeting telomeres, particularly with an agent that is also a poor Pgp substrate, should be effective against both Pgp-expressing and Pgp-nonexpressing taxane-resistant prostate cancer cells. Consistent with these observations, KML001 retains significant activity in the taxane-resistant cells, targeting both the SP and non-SP fractions (Fig 5b-d).

Although telomere lengths and telomerase activity are not affected by drug selection, importantly KML001 or KML001 in combination with paclitaxel can significantly reduce hTERT gene expression and also cause erosion of telomeres (Fig 6). Drug combination studies reveal that KML001 is synergistic with either paclitaxel or docetaxel in both taxane-resistant and *wt* DU145 cells (Fig 7, Table 2). Such synergism is also observed in the androgen-sensitive LNCaP cells, and in the androgen-insensitive LNCaP/C81 cells grown in phenol red-free media supplemented with charcoal stripped serum (i.e., androgen-deprived conditions) (Table 2).

Table 2 also lists the calculated drug reduction index (DRI) values for KML001, paclitaxel, and docetaxel in the combination regimens for the various cell lines. It is apparent from these studies

Molecular Pharmacology Fast Forward. Published on May 14, 2012 as DOI: 10.1124/mol.111.076752
This article has not been copyedited and formatted. The final version may differ from this version.

that sensitivity to the taxanes (particularly docetaxel) is significantly enhanced when they are combined with KML001. For instance, in *wt* DU145 cells the DRI value for docetaxel is 13, and in *wt* androgen-sensitive LNCaP cells it is 38 (Table 2), suggesting that anywhere from 13- to 38-fold less docetaxel can be used when combined with KML001 to produce the same treatment effect as when used alone. Although significant synergism between KML001 and paclitaxel or KML001 and docetaxel also exists in DU145/Pac200 and DU145/Doc60 cells, given their already high basal levels of resistance, and the limits imposed by the actual drug levels that can be achieved safely in the clinical setting, it would be more difficult to effectively eradicate all the highly taxane-resistant cancer cells with the combination regimens despite enhanced drug sensitivities. On the other hand, the KML001/taxane combinations are likely to be particularly useful in *wt* non-selected chemotherapy-naive prostate cancer cells given their significantly lower basal IC_{50} values for the taxanes. Based on the calculated DRI values, these drug combinations are also likely to be more effective in androgen-sensitive than in androgen-insensitive prostate cancer cells.

KML001 is an orally bioavailable trivalent arsenical compound. A paradigm for using arsenicals in clinical practice exists for another trivalent arsenical, i.e. arsenic trioxide (ATO), which is approved for patients with acute promyelocytic leukemia (APL) who relapse after initial therapies (Soignet et al., 1998; Soignet et al., 2001). ATO is also being incorporated as part of consolidation therapy for the initial treatment of APL (Powell et al., 2010). Further, a recent study has piloted the use of ATO as monotherapy for patients with newly diagnosed APL (Ghavamzadeh et al., 2011). Both apoptotic and cytodifferentiative effects have been attributed to ATO, depending upon cellular context, with IC_{50} values for various human cancer cell lines

being in the μM range (Ajana et al., 2009). Pharmacokinetic studies reveal that such plasma concentrations can be achieved in patients treated with ATO at the recommended doses for APL (Shen et al., 2001; Fox et al., 2008). The paradigm established with ATO suggests that KML001 may also potentially have a role in appropriately defined clinical settings. An ongoing phase I pharmacokinetic/pharmacodynamic study evaluating escalating doses of KML001 with fixed dose cisplatin in solid tumors is currently ongoing in the U.S. (Edelman, 2009, http://clinicaltrials.gov/ct2/show/NCT01110226).

KML001, like ATO, targets telomeres, but may also modulate other cellular functions by generating reactive oxygen species or binding to sulfhydryl groups in proteins (Miller et al., 2002; Mei et al., 2002). Regardless of its specific mode(s) of action, it is apparent that KML001/taxane combinations produce significant synergistic anti-proliferative effects in several different types of prostate cancer cell lines that potentially represent various states of the disease, including androgen-sensitive, androgen-insensitive, taxane-sensitive and taxane-resistant prostate cancers. In summary, although our results need to be extended to in vivo models in future studies, they raise the intriguing possibility that targeting telomeres with an arsenical and microtubules with a taxane may be a useful approach to improving outcomes in prostate cancer, and warrants further evaluation.

Molecular Pharmacology Fast Forward. Published on May 14, 2012 as DOI: 10.1124/mol.111.076752
This article has not been copyedited and formatted. The final version may differ from this version.

Acknowledgments

We dedicate the present study to the memory of our dear friend and colleague, Dr. Angelika Burger, who was the inspiration behind this work. Dr. Burger devoted her life to the study of cancer. Tragically, she passed away in May, 2011. Dr. Burger's wisdom, courage, grace and dedication to scientific excellence will be forever cherished.

Authorship Contributions

Participated in research design: Hussain, Zhang, Suer, Ning.

Conducted experiments: Zhang, Suer, Vemula, Adediran, Livak, Khan, Ning.

Contributed new reagents or analytic tools: Livak.

Performed data analysis: Hussain, Zhang, Suer, Livak, Khan, Ning.

Wrote or contributed to the writing of the manuscript: Hussain, Zhang, Suer, Livak.

References

Ajana I, Astier A and Gibaud S (2009) Arsthinol nanosuspensions: pharmacokinetics and anti-leukaemic activity on NB4 promyelocytic leukaemia cells. *J Pharm Pharmacol* **61:**1295-1301.

Baerlocher GM, Vulto I, de Jong G and Lansdorp PM (2006) Flow cytometry and FISH to measure the average length of telomeres (flow FISH). *Nat Protocols* **1**:2365-2376.

Berthold DR, Pond GR, Soban F, de Wit R, Eisenberger M and Tannock IF (2008) Docetaxel plus prednisone or mitoxantrone plus prednisone for advanced prostate cancer: updated survival in the TAX 327 study. *J Clin Oncol* **26:**242-245.

Burger AM and Harnden P (1998) Telomerase in germ cell tumours: inhibition of telomerase activity after cisplatin-based therapy, in *Germ Cell Tumours IV* (Jones I, Appelyard I, Harnden P and Joffe JK eds) pp 73-80, John Libbey & Co Ltd London.

Burger AM (2002) Standard TRAP assay, in *Telomeres and Telomerase: Methods in Molecular Biology* (Double JA and Thompson MJ eds) pp 109-124, The Humana Press, Totowa, New Jersey.

Burger AM, Dai F, Schultes CM, Reszka AP, Moore MJ, Double JA and Neidle S (2005) The G-quadruplex-interactive molecule BRACO-19 inhibits tumor growth, consistent with telomere targeting and interference with telomerase function. *Cancer Res* **65:**1489-1496.

Cai X, Yu Y, Huang Y, Zhang L, Jia PM, Zhao Q, Chen Z, Tong JH, Dai W and Chen GQ (2003) Arsenic trioxide-induced mitotic arrest and apoptosis in acute promyelocytic leukemia cells. *Leukemia* **17**:1333-1337.

Chou TC and Hayball MP (1977) *CalcuSyn for Windows: Multiple-Drug Dose-Effect Analyzer and Mannual*, Biosoft, Cambridge, UK.

Chou TC and Talalay P (1984) Quantitative analysis of dose-effect relationships: the combined effects of multiple drugs or enzyme inhibitors. *Adv Enzyme Regul* **22:**27-55.

Chou TC (2008) Preclinical versus clinical drug combination studies. *Leuk Lymphoma* **49:**2059-2080.

Collins AT, Berry PA, Hyde C, Stower MJ and Maitland NJ (2005) Prospective identification of tumorigenic prostate cancer stem cells. *Cancer Research* **65**:10946-10951.

d'Adda di Fagagna F, Reaper PM, Clay-Farrace L, Fiegler H, Carr P, Von Zglinicki T, Saretzki G, Carter NP and Jackson SP (2003) A DNA damage checkpoint response in telomere-initiated senescence. *Nature* **426:**194-198.

Darshan MS, Loftus MS, Thadani-Mulero M, Levy BP, Escuin D, Zhou XK, Gjyrezi A, Chanel-Vos C, Shen R, Tagawa ST, Bander NH, Nanus DM and Giannakakou P (2011) Taxane-induced blockade to nuclear accumulation of the androgen receptor predicts clinical responses in metastatic prostate cancer. *Cancer Res* **71**:6019-6029.

de Bono JS, Oudard S, Ozguroglu M, Hansen S, Machiels JP, Kocak I, Gravis G, Bodrogi I, Mackenzie MJ, Shen L, Roessner M, Gupta S and Sartor AO (2010) Prednisone plus cabazitaxel

or mitoxantrone for metastatic castration-resistant prostate cancer progressing after docetaxel treatment: a randomised open-label trial. *Lancet* **376:**1147-1154.

de Bono JS, Logothetis CJ, Molina A, Fizazi K, North S, Chu L, Chi KN, Jones RJ, Goodman OB, Saad F, Staffurth JN, Mainwaring P, Harland S, Flaig TW, Hutson TE, Cheng T, Patterson H, Hainsworth JD, Ryan CJ, Sternberg CN, Ellard SL, Flechon A, Saleh M, Scholz M, Efstathiou E, Zivi A, Bianchini D, Loriot Y, Chieffo N, Kheoh T, Haqq CM and Scher HI (2011) Abiraterone and increased survival in metastatic prostate cancer. *N Engl J Med* **364:**1995-2005.

Deschatrette J, Ng KH, Gouthiere L, Maigne J, Guerroui S and Wolfrom C (2004) Telomere dynamics determine episodes of anticancer drug resistance in rat hepatoma cells. *Anticancer Drugs* **15:**671-678.

Fizazi K, Carducci M, Smith M, Damiao R, Brown J, Karsh L, Milecki P, Shore N, Rader M, Wang H, Jiang Q, Tadros S, Dansey R and Goessl C (2011) Denosumab versus zoledronic acid for treatment of bone metastases in men with castration-resistant prostate cancer: a randomised, double-blind study. *Lancet* **377:**813-822.

Fox E, Razzouk BI, Widemann BC, Xiao S, O'Brien M, Goodspeed W, Reaman GH, Blaney SM, Murgo AJ, Balis FM and Adamson PC (2008) Phase 1 trial and pharmacokinetic study of arsenic trioxide in children and adolescents with refractory or relapsed acute leukemia, including acute promyelocytic leukemia or lymphoma. *Blood* **111:**566-573.

Gan L, Chen S, Wang Y, Watahiki A, Bohrer L, Sun Z, Wang Y and Huang H (2009) Inhibition of the androgen receptor as a novel mechanism of taxol chemotherapy in prostate cancer. *Cancer Res* **69**:8386-8394.

Ghavamzadeh A, Alimoghaddam K, Rostami S, Ghaffari SH, Jahani M, Iravani M, Mousavi SA, Bahar B and Jalili M (2011) Phase II study of single-agent arsenic trioxide for the front-line therapy of acute promyelocytic leukemia. *J Clin Oncol* **29:**2753-2757.

Goodell MA, Brose K, Paradis G, Conner AS and Mulligan RC (1996) Isolation and functional properties of murine hematopoietic stem cells that are replicating in vivo. *J Exp Med* **183:**1797-1806.

Greenberger LM and Sampath D (2006) Resistance to taxanes, in *Cancer Drug Resistance* (Teicher BA ed) pp 329-358, Humana Press, Totowa, New Jersey.

Grossi A and Biscardi M (2004) Reversal of MDR by verapamil analogues. *Hematology* **9**:47-56.

Han YH, Moon HJ, You BR, Kim SZ, Kim SH and Park WH (2010) Effects of arsenic trioxide on cell death, reactive oxygen species and glutathione levels in different cell types. *Int J Mol Med* **25:**121-128.

Ishibashi T and Lippard SJ (1998) Telomere loss in cells treated with cisplatin. *PNAS* **95:**4219-4223.

Kantoff PW, Higano CS, Shore ND, Berger ER, Small EJ, Penson DF, Redfern CH, Ferrari AC, Dreicer R, Sims RB, Xu Y, Frohlich MW and Schellhammer PF (2010) Sipuleucel-T immunotherapy for castration-resistant prostate cancer. *N Engl J Med* **363:**411-422.

Li YM and Broome JD (1999) Arsenic targets tubulins to induce apoptosis in myeloid leukemia cells. *Cancer Res* **59**:776-780.

Lin M-F, Meng T-C, Rao PS, Chang C, Schonthal AH and Lin F-F (1998) Expression of human prostatic acid phosphatase correlates with androgen-stimulated cell proliferation in prostate cancer cell lines. *J Biol Chem* **273:**5939-5947.

Ling Y-H, Jiang J-D, Holland JF and Perez-Soler R (2002) Arsenic trioxide produces polymerization of microtubules and mitotic arrest before apoptosis in human tumor cell lines. *Mol Pharmacol* **62**:529-538.

Livak KJ and Schmittgen TD (2001) Analysis of relative gene expression data using real-time quantitative PCR and the 2(-Delta Delta C(T)) Method. *Methods* **25**:402-408.

Mei N, Kunugita N, Hirano T and Kasai H (2002) Acute arsenite-induced 8-hydroxyguanine is associated with inhibition of repair activity in cultured human cells. *Biochemical and Biophysical Research Communications* **297**:924-930.

Miller WH, Jr., Schipper HM, Lee JS, Singer J and Waxman S (2002) Mechanisms of action of arsenic trioxide. *Cancer Res* **62**:3893-3903.

Mo Y, Gan Y, Song S, Johnston J, Xiao X, Wientjes MG and Au JLS (2003) Simultaneous targeting of telomeres and telomerase as a cancer therapeutic approach. *Cancer Res* **63:**579-585.

Mosmann T (1983) Rapid colorimetric assay for cellular growth and survival: application to proliferation and cytotoxicity assays. *J Immunol Methods* **65:**55-63.

Multani AS, Li C, Ozen M, Imam AS, Wallace S and Pathak S (1999) Cell-killing by paclitaxel in a metastatic murine melanoma cell line is mediated by extensive telomere erosion with no decrease in telomerase activity. *Oncol Rep* **6:**39-44.

Olaussen KA, Dubrana K, Domont J, Spano JP, Sabatier L and Soria JC (2006) Telomeres and telomerase as targets for anticancer drug development. *Crit Rev Oncol Hematol* **57:**191-214.

Patrawala L, Calhoun T, Schneider-Broussard R, Li H, Bhatia B, Tang S, Reilly JG, Chandra D, Zhou J, Claypool K, Coghlan L and Tang DG (2006) Highly purified CD44+ prostate cancer cells from xenograft human tumors are enriched in tumorigenic and metastatic progenitor cells. *Oncogene* **25**:1696-1708.

Petrylak DP, Tangen CM, Hussain MH, Lara PN, Jones JA, Taplin ME, Burch PA, Berry D, Moinpour C, Kohli M, Benson MC, Small EJ, Raghavan D and Crawford ED (2004) Docetaxel and estramustine compared with mitoxantrone and prednisone for advanced refractory prostate cancer. *N Engl J Med* **351:**1513-1520.

Phatak P, Dai F, Butler M, Nandakumar MP, Gutierrez PL, Edelman MJ, Hendriks H and Burger AM (2008) KML001 cytotoxic activity is associated with its binding to telomeric sequences and telomere erosion in prostate cancer cells. *Clin Cancer Res* **14:**4593-4602.

Powell BL, Moser B, Stock W, Gallagher RE, Willman CL, Stone RM, Rowe JM, Coutre S, Feusner JH, Gregory J, Couban S, Appelbaum FR, Tallman MS and Larson RA (2010) Arsenic trioxide improves event-free and overall survival for adults with acute promyelocytic leukemia: North American Leukemia Intergroup Study C9710. *Blood* **116:**3751-3757.

Reya T, Morrison SJ, Clarke MF and Weissman IL (2001) Stem cells, cancer, and cancer stem cells. *Nature* **414:**105-111.

Shen Y, Shen ZX, Yan H, Chen J, Zeng XY, Li JM, Li XS, Wu W, Xiong SM, Zhao WL, Tang W, Wu F, Liu YF, Niu C, Wang ZY, Chen SJ and Chen Z (2001) Studies on the clinical efficacy and pharmacokinetics of low-dose arsenic trioxide in the treatment of relapsed acute promyelocytic leukemia: a comparison with conventional dosage. *Leukemia* **15:**735-741.

Smith V, Dai F, Spitz M, Peters GJ, Fiebig HH, Hussain A and Burger AM (2009) Telomerase activity and telomere length in human tumor cells with acquired resistance to anticancer agents. *J Chemother* **21:**542-549.

Soignet SL, Maslak P, Wang ZG, Jhanwar S, Calleja E, Dardashti LJ, Corso D, DeBlasio A, Gabrilove J, Scheinberg DA, Pandolfi PP and Warrell RP (1998) Complete remission after treatment of acute promyelocytic leukemia with arsenic trioxide. *N Engl J Med* **339:**1341-1348.

Soignet SL, Frankel SR, Douer D, Tallman MS, Kantarjian H, Calleja E, Stone RM, Kalaycio M, Scheinberg DA, Steinherz P, Sievers EL, Coutre S, Dahlberg S, Ellison R and Warrell RP, Jr. (2001) United States multicenter study of arsenic trioxide in relapsed acute promyelocytic leukemia. *J Clin Oncol* **19:**3852-3860.

Stuelten CH, Mertins SD, Busch JI, Gowens M, Scudiero DA, Burkett MW, Hite KM, Alley M, Hollingshead M, Shoemaker RH and Niederhuber JE (2010) Complex display of putative tumor stem cell markers in the NCI60 tumor cell line panel. *Stem Cells* **28:**649-660.

Tang Y, Khan MA, Goloubeva O, Lee DI, Jelovac D, Brodie AM and Hussain A (2006) Docetaxel followed by castration improves outcomes in LNCaP prostate cancer-bearing severe combined immunodeficient mice. *Clin Cancer Res* **12:**169-174.

Tannock IF, de Wit R, Berry WR, Horti J, Pluzanska A, Chi KN, Oudard S, Theodore C, James ND, Turesson I, Rosenthal MA and Eisenberger MA (2004) Docetaxel plus prednisone or mitoxantrone plus prednisone for advanced prostate cancer. *N Engl J Med* **351:**1502-1512.

Tsuruo T, Iida H, Tsukagoshi S and Sakurai Y (1981) Overcoming of vincristine resistance in p388 leukemia in vivo and in vitro through enhanced cytotoxicity of vincristine and vinblastine by verapamil. *Cancer Res* **41**:1967-1972.

Visvader JE and Lindeman GJ (2008) Cancer stem cells in solid tumours: accumulating evidence and unresolved questions. *Nat Rev Cancer* **8:**755-768.

Zhu M-L, Horbinski CM, Garzotto M, Qian DZ, Beer TM and Kyprianou N (2010) Tubulin-targeting chemotherapy impairs androgen receptor activity in prostate cancer. *Cancer Res* **70**:7992-8002.

Molecular Pharmacology Fast Forward. Published on May 14, 2012 as DOI: 10.1124/mol.111.076752
This article has not been copyedited and formatted. The final version may differ from this version.

Footnotes

This work was supported by Dept of Defense [Grants PC081047, A.B.]; and a Merit Review Award, Medical Research Service, Dept of Veterans Affairs [A.H.]. S.S. was supported in part by a grant from Komipharm International Co.

B.Z. and S.S. contributed equally to this work.

Address Correspondence to: Dr. Arif Hussain, University of Maryland Greenebaum Cancer Center, 22 S. Greene St, Baltimore, MD 21201. Email: ahussain@som.umaryland.edu

Molecular Pharmacology Fast Forward. Published on May 14, 2012 as DOI: 10.1124/mol.111.076752
This article has not been copyedited and formatted. The final version may differ from this version.

Legends for figures

Fig 1. Pgp and BCRP expression in prostate cancer cells. A. Western blot. Relative expression of Pgp and BCRP in DU145-derived cell lines. Whole-cell extracts were isolated in modified RIPA buffer and 50 µg total protein loaded per lane. Western blots are representative of at least three independent experiments. B. Flow Cytomety. Cell surface expression of Pgp and BCRP in *wt* and taxane-resistant cells. 0.5 x 10^6 cells were stained with antibodies as indicated for 30 minutes in the dark. FACS analysis was carried out with 10,000 events recorded for each sample. These experiments were repeated three independent times. Shown are PE (Phycoerythrin)- or FITC-isotype stained cells (white; control) and PE-Pgp or FITC-BCRP positive cells (grey). C. Western blot. Pgp and BCRP expression in LNCaP and LNCaP/C81 cells. 50 µg total protein loaded per lane.

Fig 2. Flow cytometry. DU145 *wt* and DU145/Doc cells (0.5 x 10^6) were resuspended in pre-warmed DMEM/F12 medium with Hoechst 33342 in the absence (A) or presence of verapamil (B; Pgp inhibitor) or K0143 (C; BCRP inhibitor). The cells were incubated in 37°C water bath for 90 minutes. FACS analysis was carried out after washing cells in cold HBSS. Numbers in the dotted box represent the proportion of cells (designated 'side population' [SP]) that do not take up Hoechst 33342 due to the vital dye being extruded out of the cells by Pgp. The data shown are representative of at least four independent experiments.

Fig 3. Immunostaining and flow cytometry. DU145 *wt* and DU145/Doc60 cells (0.5x10^6) were resuspended in HBSS+ medium, stained with APC anti-CD44, PE anti-CD133 and their

Molecular Pharmacology Fast Forward. Published on May 14, 2012 as DOI: 10.1124/mol.111.076752
This article has not been copyedited and formatted. The final version may differ from this version.

respective control isotypes. The cells were incubated on ice for 30 minutes in the dark. FACS analysis was carried out after washing cells in cold HBSS+. The numbers reflect the proportion of cells positive for surface CD44 or CD133 compared to isotype controls. The data shown are representative of at least three independent experiments.

Fig 4. Analysis of DU145/Pac200 cells sorted by flow cytometry. A. Upper Panel. Hoechst 33342 uptake by DU145/Pac200 cells in the absence or presence of verapamil. Lower Panel. Cells sorted by gating relative to the verapamil (VP)-suppressible fraction into SP+ and SP- cells were re-analyzed via FACS. B. Western blot. Pgp expression in DU145/Pac200 cells and the sorted SP+ and SP- cell fractions. 1 μg total protein loaded per lane. C. MTT assay. DU145, DU145/Pac200, and SP+ and SP- fractions analyzed by MTT assay as described under *Material and Methods*. D. Flow cytometry. Upper panel. Cell surface expression of Pgp using isotype- or Pgp-specific antibody. Lower panel. Cells sorted according to whether or not they express cell surface Pgp. E. MTT assay. DU145, DU145/Pac200, and Pgp+ and Pgp- fractions analyzed by MTT assay.

Fig 5. Effects of KML001 and taxanes on prostate cancer cells. A. DU145 cells. Side population (SP) assay. Top: cells stained with Hoechst 33342. Middle: cells treated with paclitaxel at IC_{50} or IC_{100} for 72 hours prior to Hoechst 33342 staining. Bottom: cells treated with KML001 at IC_{50} or IC_{100} for 72 hours prior to Hoechst 33342 staining. B. DU145/Pac200 cells. MTT assay. Growth inhibition of DU145/Pac200 cells and the SP and non-SP fractions by KML001. C. DU145/Pac200 cells. Immunoflourescence. γ-H2AX foci formation (green) in DU145/PacSP- and SP+ populations treated with vehicle (control) or KML001 at IC_{100} for 24 hours. Shown are

Molecular Pharmacology Fast Forward. Published on May 14, 2012 as DOI: 10.1124/mol.111.076752
This article has not been copyedited and formatted. The final version may differ from this version.

representative examples from 10-15 independent images. D. Mean signal intensity of γ-H2AX foci from at least 100 nuclei per experiment in DU145, DU145/Pac200 and SP+ and SP- fractions.

Fig 6. Telomerase gene expression and analysis of telomere lengths. A. Real time PCR. hTERT mRNA expression was evaluated in DU145/Pac200 cells that were treated for 72 hours with KML001, paclitaxel, or both drugs at their IC_{50} concentrations. The experiments were done in triplicates. B. Metaphase spread. Detection of telomeres by the PNA TelC-FAM probe in DU145 cells. C. Flow FISH. Fluorescence histograms (in triplicates) are shown for DU145 cells treated with KML001, paclitaxel, or KML001 plus paclitaxel at IC_{50} concentrations for 72 hours and then hybridized in situ with PNA TelC-FAM probe. D. Telomere length for each sample was calculated from the fluorescence histograms after subracting background mean fluorescence intensity (MFI; no probe) from MFI obtained upon hydrization with PNA TelC-FAM probe.

Fig 7. Combination index (CI) values for DU145/Pac200 cells as a function of cell fraction affected. Upper. KML001 plus paclitaxel. Lower. KML001 plus docetaxel. 4000 cells/well were plated in 96 well plates. Following overnight incubation, a serial dilution of single drug or two-drug combinations at their fixed IC_{50} ratios was added to each well and incubated for 5 days. MTT assay was done and CI was determined using CalcuSyn software.

Molecular Pharmacology Fast Forward. Published on May 14, 2012 as DOI: 10.1124/mol.111.076752
This article has not been copyedited and formatted. The final version may differ from this version.

Table 1. Drug Sensitivities, Telomere Lengths and Telomerase Activity of Various Prostate Cancer Cell Lines

	Paclitaxel		**Docetaxel**		**KML001**		
Cell lines	IC_{50} (μM)*	Fold Resistance	IC_{50} (μM)*	Fold Resistance	IC_{50} (μM)*	TA Ratio	Mean TRF (kb)
DU145 WT	0.00250 ± 0.00015	1	0.0005 ± 0.0001	1	4.5 ± 1.0	1.00	2.5
DU145/Pac1	0.006 ± 0.002	2.4	0.001 ± 0.001	2	ND	ND	ND
DU145/Pac10	0.060 ± 0.009	24	0.050 ± 0.017	100	9.3 ± 2.1	0.98	2.0
DU145/Pac200	0.35 ± 0.08	140	0.2 ± 0.1	400	13.3 ± 2.0	1.07	3.0
DU145/Doc1	0.0020 ± 0.0003	1	0.001 ± 0.001	2	ND	ND	ND
DU145/Doc10	0.060± 0.007	24	0.050 ± 0.004	100	8.5 ± 4.1	1.07	3.5
DU145/Doc60	0.25 ± 0.05	100	0.250 ± 0.009	500	5.6 ± 2.9	0.96	2.9
LNCaP	0.00025± 0.00011	1	0.00020 ± 0.00012	1	3.6 ± 1.4	1.18	2.5
LNCaP/C81	0.0010 ± 0.0002	4	0.00040 ± 0.00023	2	2.3 ± 0.8	1.10	2.7

* IC_{50} values (mean ± SD, μM) based on three independent experiments
TA: Telomerase activity; TA ratio with respect to DU145 cells
TRF: Telomere restriction fragment
ND: Not determined

Molecular Pharmacology Fast Forward. Published on May 14, 2012 as DOI: 10.1124/mol.111.076752
This article has not been copyedited and formatted. The final version may differ from this version.

Table 2. Combination Index and Drug Reduction Index Values for KML001/Taxane Combinations

	KML001 Plus Paclitaxel				**KML001 Plus Docetaxel**			
Cell lines	FA	CI	DRI KML	DRI Pac	FA	CI	DRI KML	DRI Doc
DU145	0.50	0.835	2.328	2.466	0.50	0.805	1.375	12.791
	0.75	0.681	2.432	3.699	0.75	0.922	1.186	12.732
	0.90	0.574	2.541	5.550	0.90	1.056	1.023	12.673
DU145/Pac200	0.50	0.470	6.529	3.156	0.50	0.792	1.514	7.637
	0.75	0.407	6.674	3.892	0.75	0.859	1.370	7.736
	0.90	0.355	6.821	4.800	0.90	0.934	1.240	7.837
DU145/Doc60	0.50	1.106	0.985	11.008	0.50	0.954	1.116	17.219
	0.75	0.877	1.303	9.148	0.75	0.766	1.389	21.722
	0.90	0.711	1.724	7.602	0.90	0.615	1.728	27.403
LNCaP	0.50	0.559	1.944	22.549	0.50	0.341	3.184	37.737
	0.75	0.684	1.561	23.199	0.75	0.337	3.214	38.352
	0.90	0.839	1.255	23.868	0.90	0.334	3.243	38.976
LNCaP/C81	0.50	1.640	2.574	0.799	0.50	0.403	7.329	3.745
	0.75	0.790	3.242	2.079	0.75	0.603	3.966	2.846
	0.90	0.430	4.084	5.407	0.90	0.928	2.146	2.163

FA: Fraction affected
CI: Combination index
DRI: Drug reduction index

Figure 1

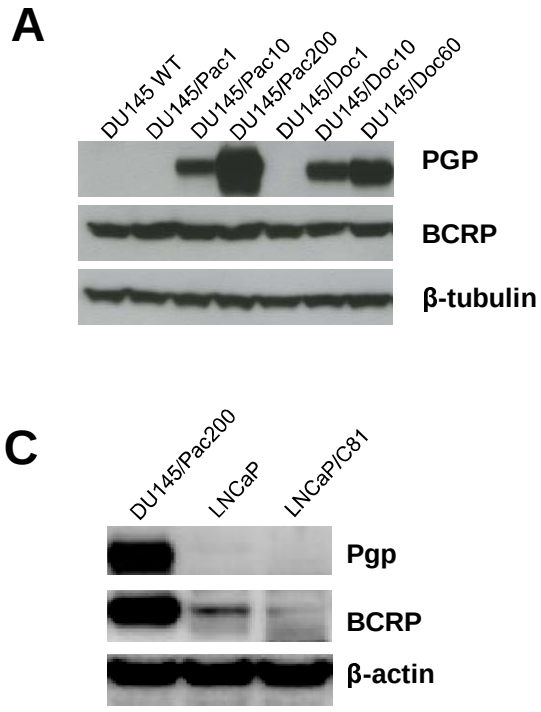

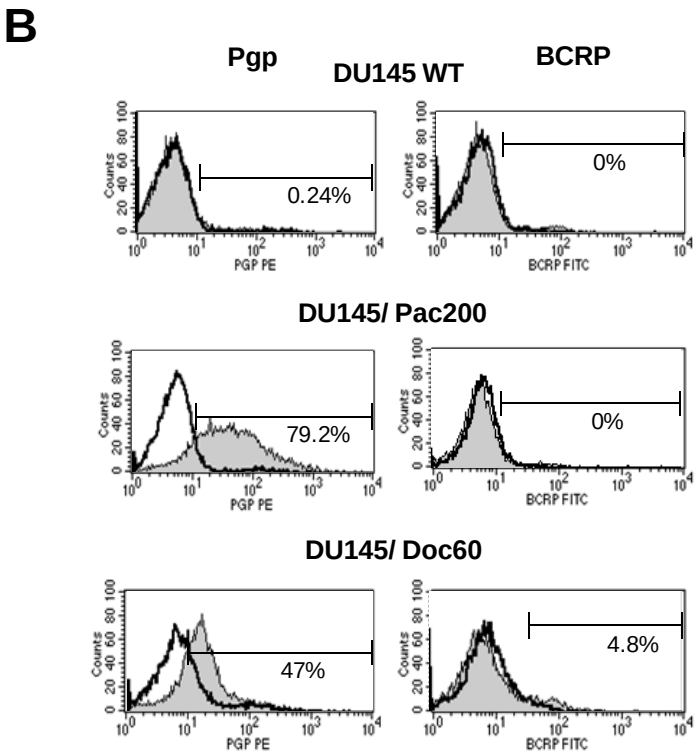

Figure 2

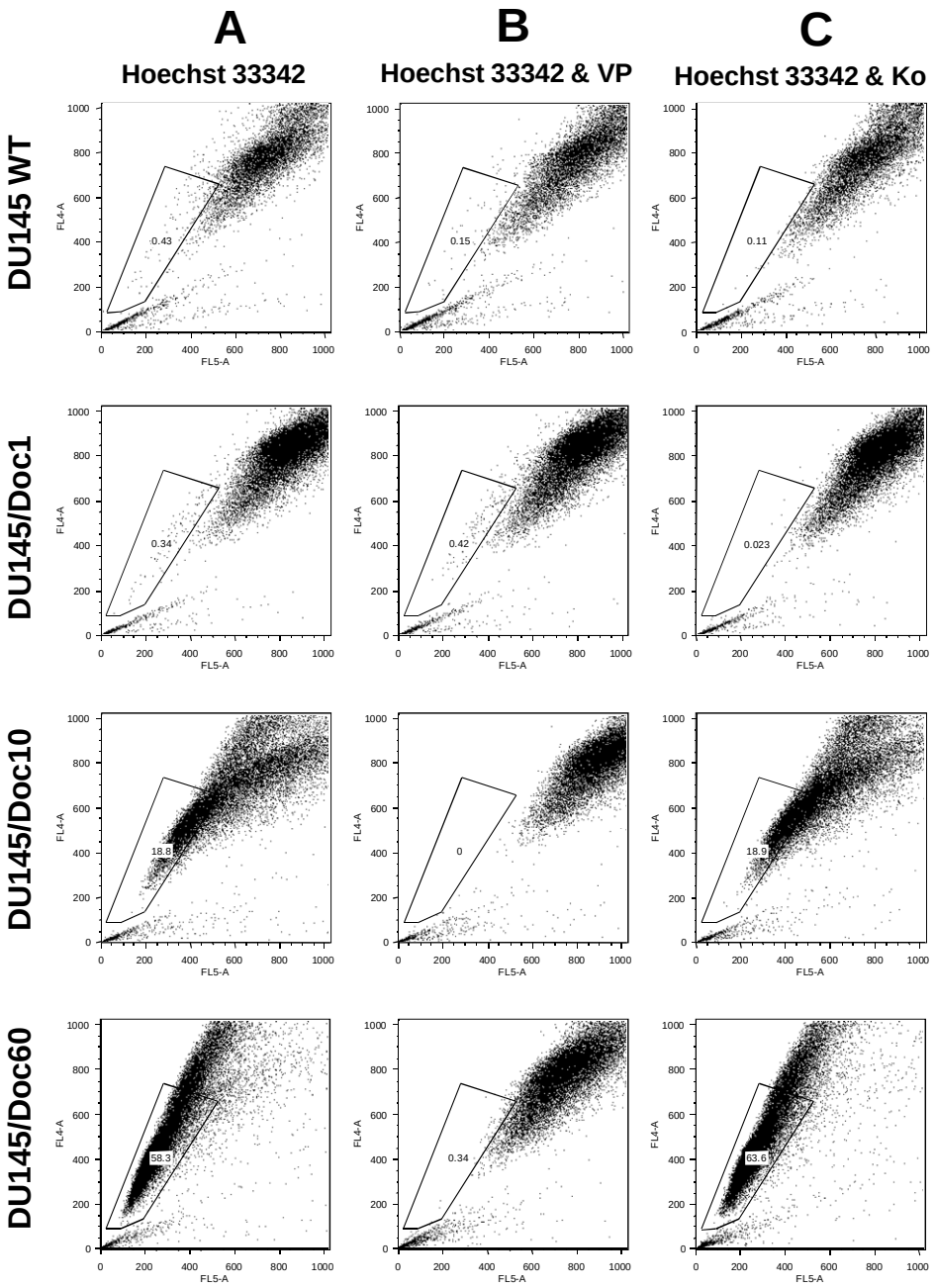

Figure 3

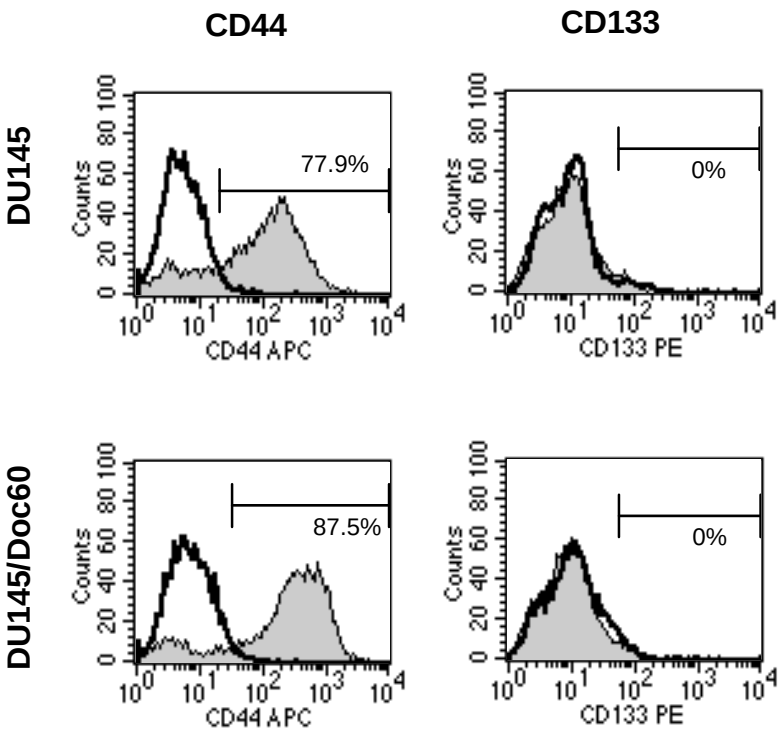

Figure 4

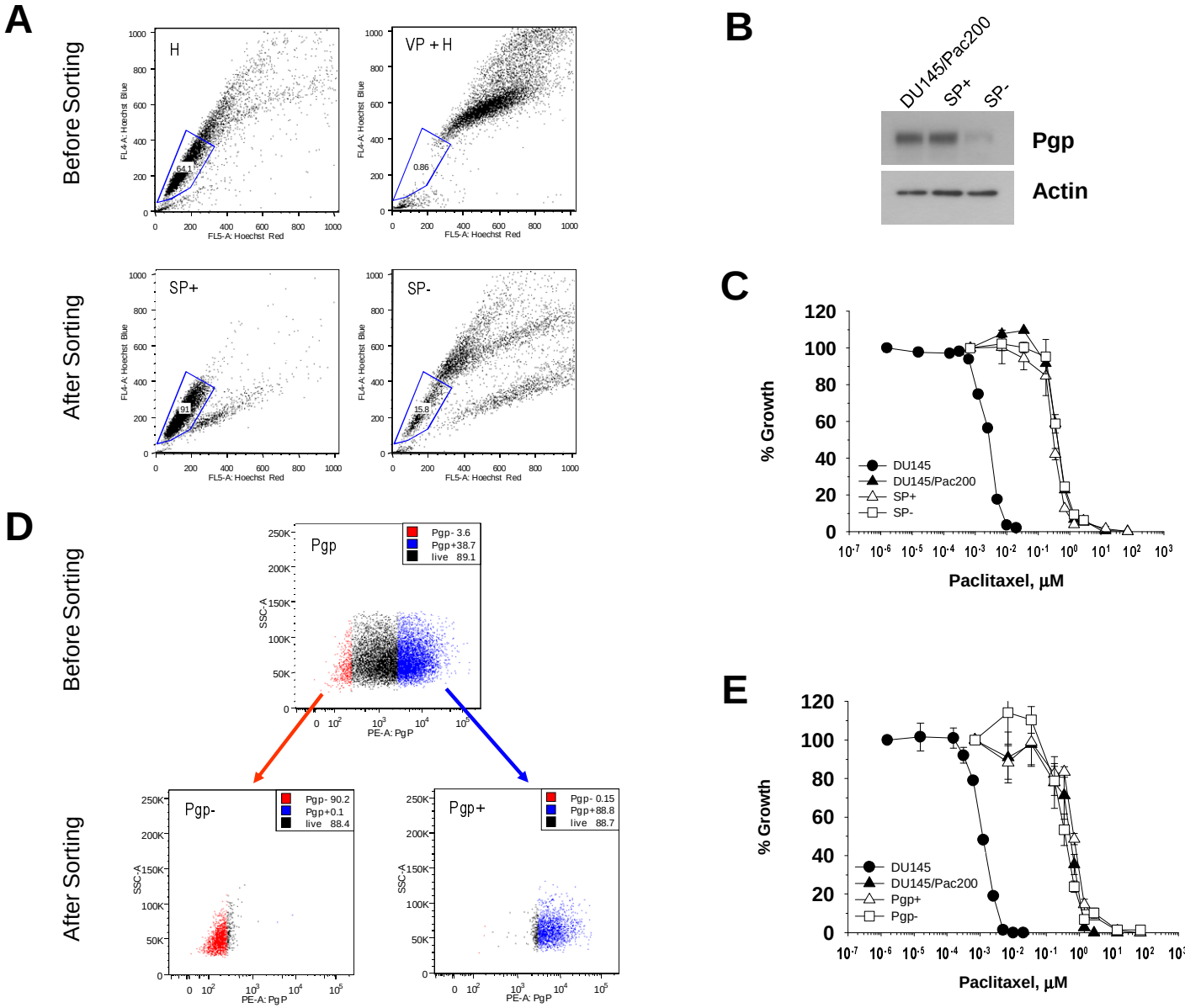

Figure 5

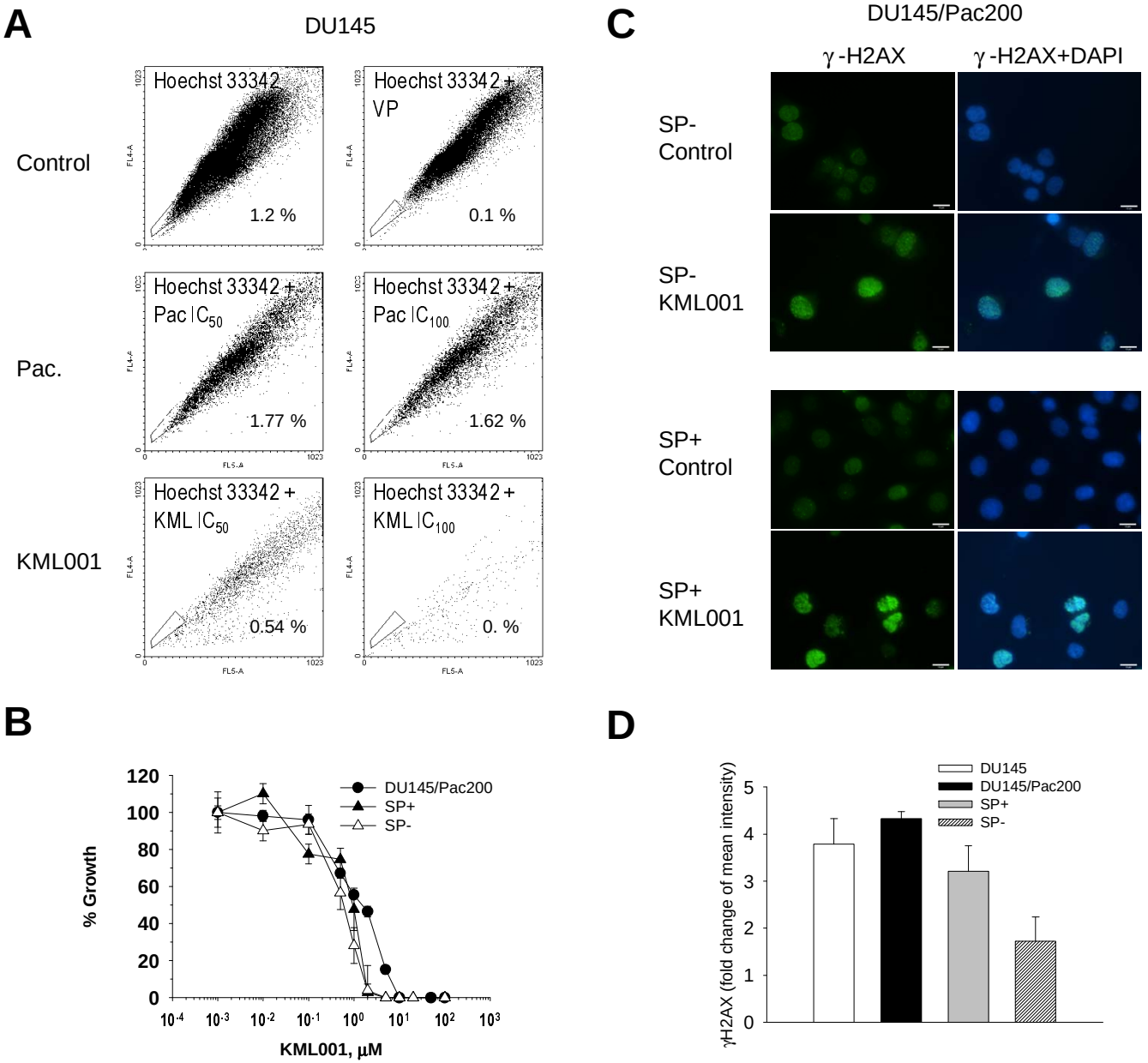

Figure 6

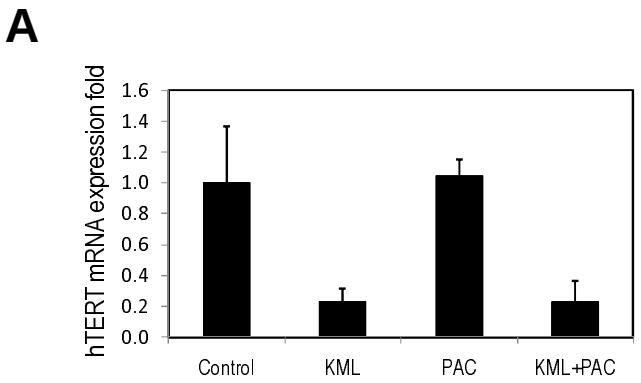

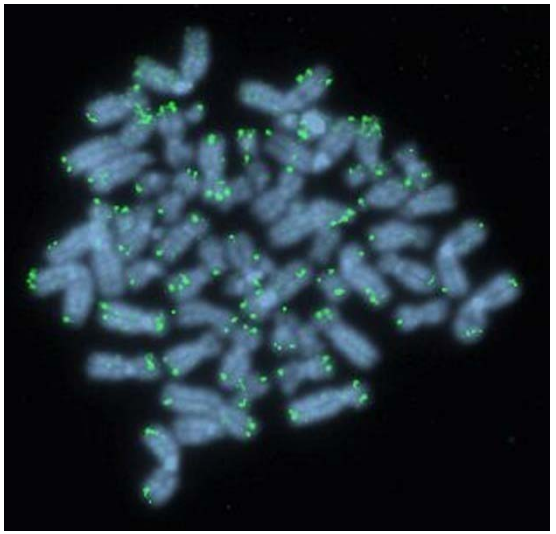

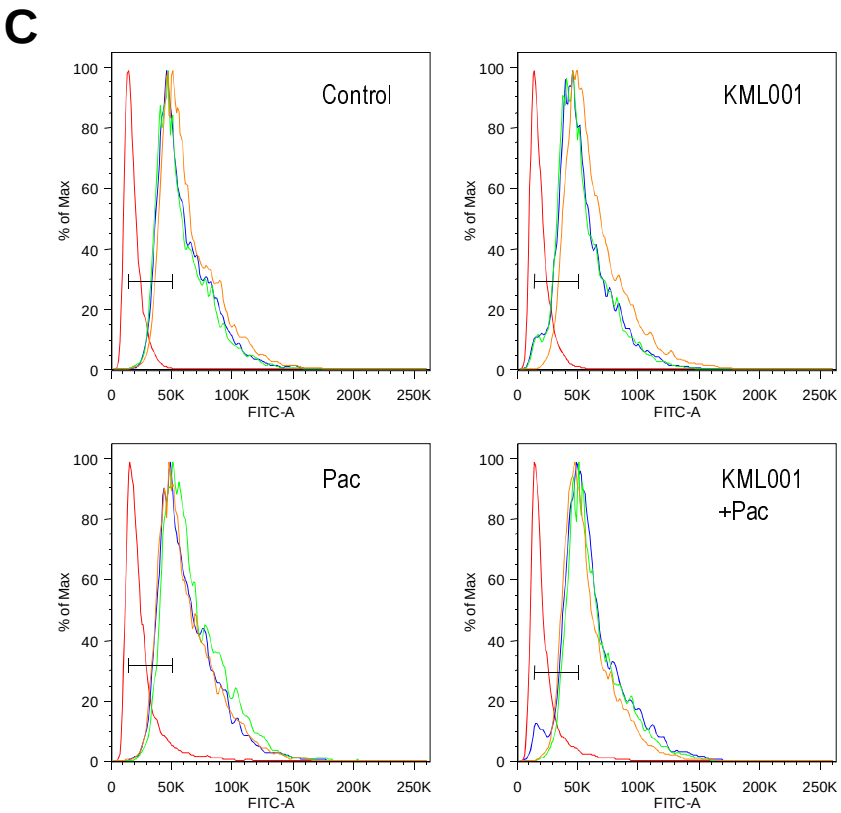

D

DU145	Telomere Fluorescence (Mean ± SD)	Telomere Length (Kb) (Mean ± SD)
Control	47041 ± 3970	2.50 ± 0.21
KML001	38662 ± 2724	2.05 ± 0.14
Paclitaxel	46145 ± 3560	2.45 ± 0.19
KML + Pac	36781 ± 4130	1.95 ± 0.22

Figure 7